Equalizers for Multi-scale/Multi-lag Wireless Channels

Urbashi Mitra[*] and Geert Leus[†]

[*] Ming Hsieh Department of Electrical Engineering, University of Southern California, USA, ubli@usc.edu
[†] Fac. of Electrical Engineering, Delft University of Technology, the Netherlands, g.j.t.leus@tudelft.nl

Abstract—**Equalizer designs for digital communications over wireless channels exhibiting both multi-lag and multi-scale are investigated. Such channel models are well-suited for underwater acoustic communications and may have impact on the design of systems for vehicle-to-vehicle communications. First, the implications of the multi-scale, multi-lag model on equalizer design are highlighted. In particular, equalizers are time-varying as a function of symbol index. Three suboptimal, low complexity block equalizers (partial, truncated, and path-combining) are compared to that of the full block equalizer and shown to offer a good tradeoff between complexity and performance. These four equalizers significantly outperform a simple matched filter which performs no equalization.**

I. INTRODUCTION

Design of digital communication systems for underwater acoustic communication has recently gained increased interest. Due to the nature of underwater signal propagation, acoustic channels differ fundamentally from terrestrial radio channels, thus requiring new transceiver designs. In particular, underwater acoustic communication systems are *wideband* in nature and time-varying. We will employ channel models which reflect the multi-scale, multi-lag nature of the wideband underwater acoustic propagation. The following works, among others, point to the multiple Doppler scale model (and hence wideband, multi-scale model) as being more accurate [1]–[4] than that typically considered for underwater acoustic communication.

There have been recent efforts devoted to developing signal representations for time-varying signals using scale-lag characterizations see *e.g.* [5]–[7]. *We underscore that there has been extensive research on the design of equalizers for time-varying narrowband channels – we do not attempt to summarize such efforts herein. We focus on equalizer designs for the multi-scale, multi-lag (MSML) channel model.* While [6], [7] studied the wideband scattering function, which is the result of the optimal matched filter receiver for the transmission of a **single, isolated** pulse, the examination of receiver designs for the transmission of a *block* of symbols does not appear to have been examined; it is this problem that we examine herein. We note that multi-scale Wiener filters were developed in [8] for linear time-invariant multipath channels for non-stationary,

multi-scale input signals. In contrast, our channels exhibit the multi-scale feature.

The Doppler scaling effect typically studied in underwater acoustic communications is the introduction of inter-carrier interference in orthogonal frequency division multiplexing (OFDM); resampling is commonly employed to mitigate this effect. However, resampling is only optimal when there is a single Doppler scale. In [9], [10], we characterized the optimal resampling for multi-scale, multi-lag channels and developed a blind estimation algorithm for the optimal resampling parameter.

Although our primary motivation is the design of transceivers for underwater acoustic communications, our resulting designs have potential application in vehicle-to-vehicle (V2V) communication systems. Recent experimental work (see *e.g.* [11], [12]) clearly shows that each path in most wireless vehicular environments has its own unique Doppler spectrum which is characterized by a completely distinct maximum Doppler shift.

One of the main contributions of this work is to highlight the need for new designs for equalizers for the multi-scale, multi-lag channel and examine the impact of the channel model on the equalizer structure. Several classical approaches are investigated for the new channel model. Three suboptimal equalizer structures, the partial, truncated, and path-combining block equalizers are shown to provide a good tradeoff between complexity and performance when compared to the full block equalizer. As shown in the numerical results, all four of these equalizers offer a measureable improvement in performance over the case of no equalization, *i.e.* a simple matched filter. The truncated block equalizer offers near full block equalizer performance at the expense of more complexity than the other two sub-optimal equalizers.

The rest of this paper is organized as follows. The signal model is presented in Section II and the implications of this model on equalizer design summarized in Section III. Equalizer designs for the multi-scale multi-lag channel are provided in Section IV and their performance examined numerically in Section V. Section VI concludes the paper.

II. SIGNAL MODEL

We adopt the scaling notation of [6], that is, a signal, $s(t)$, transmitted by a moving object over a wideband propagation medium is received as

$$r(t) = \sqrt{|a|}s(a(t - \tau)), \qquad (1)$$

where a is the Doppler scaling. If the velocity of the transmitter is v and c is the speed of the communication medium[1], then $a \approx 1 + \frac{2v}{c}$. The propagation delay is given by $\tau = \frac{d}{c}$, where d is the transmission range. When the Doppler scale is such that $a > 1$, then the scatterer is approaching the transmitter and the transmitted signal is compressed with respect to time; in contrast, when $0 < a < 1$, the received signal is dilated and the scatterer is moving away from the transmitter[2].

In our multi-scale, multi-lag channel model, multiple paths will individually scale the received signal as described in (1). The complex, baseband, received signal at the destination is given by,

$$r(t) = \sum_{m=0}^{M-1} b(m)q_m(t) + n(t) \tag{2}$$

$$q_m(t) = \sum_{l=1}^{L} v_m^l(t) \tag{3}$$

$$v_m^l(t) = h_l\sqrt{a_l}p\left(a_l(t - \tau_l) - m\frac{T}{a_l}\right)$$
$$\times e^{j2\pi f_c((a_l-1)t - a_l\tau_l)}, \tag{4}$$

where L is the number of paths and a_l, τ_l, and h_l are the Doppler scaling, delay and tap coefficient, respectively for path l and are assumed known. The packet, or block size, is given by the integer, M. The transmitted pulse shape is $p(t)$ and is assumed to have support on $[0, T)$ and be of unit energy. The transmitted data sequence is denoted by $b(m)$ assumed to be PSK and equally likely, i.i.d., the original symbol duration is T, and the associated carrier frequency of the transmitted signal is f_c. The noise process, $n(t)$ is modeled as a white, Gaussian random process. The function, $q_m(t)$ is then the effective channel function for symbol m, whereas the $v_m^l(t)$ are the contributions to $q_m(t)$ due to path l.

The channel coefficients will be modeled as Rayleigh, and independent from path to path. Future research will examine the design of channel estimation and adaptive equalizers for this time-varying environment. In the current study, we seek to determine the performance limits of practical processing.

III. IMPLICATIONS OF MULTI-SCALE, MULTI-LAG MODEL

We first observe that the support of the effective channel function $q_m(t)$ changes with the symbol index, m and thus so does the effective channel memory. In fact, if at least one of the Doppler scalings induces dilation ($a_l < 1$ for some value of l), then the support is increasing with time. The support of $q_m(t)$ is given by

$$\mathcal{T}_m = \left(\min_l\left(\frac{(m-1)T}{a_l} + \tau_l\right), \max_l\left(\frac{mT}{a_l} + \tau_l\right)\right] \tag{5}$$

If the Doppler spread is significant, then it is possible for the contributions due to individual paths, of a particular symbol

[1]For example, the speed of light is 3×10^8 m/s, whereas the speed of sound in water is 1500 m/s.

[2]For the underwater acoustic communication application it is possible that $v > c$ and thus a could be positive or negative; however, for exposition we will maintain the convention that $a > 0$.

index m, to be mutually orthogonal in time. This time-varying memory is irrespective of the delays of the individual multipath. *Thus, any traditional equalizer, optimized according to some metric, would be time-varying as a function of the symbol index of interest.* If the Doppler shifts per path were common ($a_l = a, \quad \forall\ l$), then the memory of the effective channel would be fixed and due to a combination of the multipath delays and the common Doppler scale. Finally, we observe that even if all path delays were zero ($\tau_l = 0, \quad \forall\ l$), one would still need to perform equalization due to the ISI induced by the Doppler scaling.

IV. MSML EQUALIZER DESIGNS

Herein we examine equalizer structures for sequence $\mathbf{b} \doteq [b(0), b(1), \ldots, b(M-1)]^T$. We shall focus on minimum mean squared error (MMSE) equalizers. To compute the probability of error conditioned on the channel $\mathbf{h} \doteq [h_1, h_2, \ldots, h_L]^T$ for BPSK modulation, we shall treat the residual interference after equalization as colored Gaussian noise [13]. Let $\mathbf{P}$ be a general equalizer that we apply to a set of measurements $\mathbf{y}$. Then we observe that due to the use of linear equalization, we can write the equalized signal as follows,

$$\mathbf{Py} = \mathbf{Bb} + \mathbf{w} \tag{6}$$
$$\mathbf{w} \sim \mathcal{N}\left(\mathbf{0}, \sigma^2\mathbf{W}\right). \tag{7}$$

If we now define $\bar{\mathbf{B}} \doteq \mathbf{B} - \mathbf{B}_D$, where $\mathbf{B}_D$ is the matrix comprised only of the diagonal elements of $\mathbf{B}$ along the diagonal, then the conditional probability of error is given by

$$P_e\left(m|\mathbf{h}\right) = Q\left(\sqrt{\frac{|\mathbf{B}(m,m)|^2}{\bar{\mathbf{B}}\bar{\mathbf{B}}^H(m,m) + \sigma^2\mathbf{W}(m,m)}}\right), \tag{8}$$

where $Q(x) = \frac{1}{\sqrt{2\pi}}\int_x^\infty e^{\frac{-t^2}{2}}dt$. The probability of error is determined by averaging over the complex Gaussian channel gains, $\mathbf{h}$. We underscore that the equalizer structures developed in the sequel are dependent on knowledge of the channel parameters, though this dependence is notationally suppressed in order to preserve clarity.

A. Full Block Equalizer

A set of sufficient statistics for the demodulation of $\mathbf{b}$ is formed by matched filtering the received signal with the *effective channel* associated with each symbol, that is,

$$y(m) = \int q_m^*(t)r(t)dt. \tag{9}$$

Defining $\mathbf{y} \doteq [y(0), y(1), \ldots, y(M-1)]^T$, we then obtain

$$\mathbf{y} = \mathbf{Rb} + \mathbf{n}, \quad \mathbf{R}(i,j) = \int q_i^*(t)q_j(t)dt, \tag{10}$$

where $\mathbf{n} \sim \mathcal{CN}\left(\mathbf{0}, \sigma^2\mathbf{R}\right)$; the noise is a zero-mean, complex Gaussian noise vector with covariance $\sigma^2\mathbf{R}$. The data vector is straightforwardly equalized using the standard MMSE equalizer, with the following matrices required for probability of

error computation in (8):

$$\mathbf{P}^{FB} = \left(\mathbf{R} + \sigma^2 \mathbf{I}\right)^{-1} \tag{11}$$

$$\mathbf{B}^{FB} = \left(\mathbf{I} + \sigma^2 \mathbf{R}^{-1}\right)^{-1} \tag{12}$$

$$\mathbf{W}^{FB} = \left(\mathbf{R} + \sigma^2 \mathbf{I}\right)^{-1} \mathbf{R} \left(\mathbf{R} + \sigma^2 \mathbf{I}\right)^{-1}. \tag{13}$$

While the full block equalizer requires a matrix inversion of dimension $M \times M$, as the correlation matrix is banded, lower complexity implementations of the exact full block equalizer are possible by adapting the methods of [14] to the current scenario.

B. Partial Block Equalizer

To reduce the complexity associated with the full-block equalizer we consider partially truncating the matched filters associated with the demodulation of symbol m. The key window is determined by the non-zero support of the effective channel associated with the symbol of interest, m, $\mathcal{T}_m$ defined in (5). Due to the fact that the received signal is filtered with partial effective channel functions, we connote this equalizer as the *partial block equalizer.*

We first determine the set of symbols whose effective channels have some support in the interval $\mathcal{T}_m$:

$$\mathcal{M}_m = \{\forall\, i : \exists\, t \;\ni q_i(t) \neq 0 \;\; t \in \mathcal{T}_m\}. \tag{14}$$

For the sequel, we observe that $\mathcal{M}_m$ can be written as $\mathcal{M}_m = \left\{k : k_m^{min} \leq k \leq k_m^{max}\right\}$ thereby forming a closed interval[3].

We then form the potentially truncated versions of the effective channel functions:

$$\tilde{q}_k(t) = q_k(t) I_{t \in \mathcal{T}_m}, \quad k \in \mathcal{M}_m, \tag{15}$$

where $I_{t \in \mathcal{T}_m}$ is the indicator function: it is equal to zero for $t \notin \mathcal{T}_m$ and unity for $t \in \mathcal{T}_m$. Then, the partial channel correlation matrix for symbol m is given by

$$\tilde{\mathbf{R}}_m(i - k_m^{min} + 1, k - k_m^{min} + 1)$$
$$= \int \tilde{q}_i^*(t)\tilde{q}_k(t)dt \;\; i,k \in \mathcal{M}_m. \tag{16}$$

Let $\tilde{\mathbf{b}}_m = [b(k_m^{min}),\ldots,b(k_m^{max})]^T$. The received signal $r(t)$ is matched filtered with the possibly truncated effective channel functions $\tilde{q}_k(t), \quad k \in \mathcal{M}_m$, yielding the statistics vector,

$$\tilde{\mathbf{y}}_m = \tilde{\mathbf{R}}_m \tilde{\mathbf{b}}_m + \tilde{\mathbf{n}}_m \quad \tilde{\mathbf{y}}_m(k) = \int \tilde{q}_k^*(t)r(t)dt \; k \in \mathcal{M}_m$$

where $\tilde{\mathbf{n}}_m \sim \mathcal{CN}\left(\mathbf{0}, \sigma^2 \tilde{\mathbf{R}}_m\right)$; the noise is a zero-mean, complex Gaussian noise vector with covariance $\sigma^2 \tilde{\mathbf{R}}_m$.

The MMSE equalizer has the same form as the full-block equalizer except that the correlation matrices change, that is $\mathbf{R}_m$ is replaced by $\tilde{\mathbf{R}}_m$ in (11). A similar substitution is done for computing the matrices needed to determine the performance (see (12) and (13)) and the index of interest is modified from m to $m^* = m - k_m^{min} + 1$ in (8).

[3]For the case of $\tau_l = 0, \;\; \forall l$, it is straightforward to show that $k_m^{min} = \lceil \frac{a_L(m-1) + a_1 a_L}{a_1} \rceil$ and $k_m^{max} = \min\left(M, \lceil \frac{a_1 m}{a_L}\rceil\right)$.

C. Truncated Block Equalizer

To determine the *truncated block equalizer*, we truncate the *matched filter outputs* instead of the time-domain signal as in the partial block equalizer. The memory of interest remains the same: defined by k_{min} and k_{max} as above. Adopting Matlab notation, we form the following truncated matrices and vectors:

$$\mathbf{y}_m' = \left[\mathbf{y}(k_m^{min}),\ldots,\mathbf{y}(k_m^{max})\right]^T \tag{17}$$

$$\mathbf{R}_m' = \mathbf{R}\left(k_m^{min} : k_m^{max}, :\right) \tag{18}$$

$$\rightarrow \quad \mathbf{y}_m' = \mathbf{R}_m'\mathbf{b} + \mathbf{n}_m' \tag{19}$$

$$\mathbf{n}_m' \sim \mathcal{CN}\left(\mathbf{0}, \sigma^2 \mathbf{R}_m^t\right) \tag{20}$$

$$\mathbf{R}_m^t = \mathbf{R}\left(k_m^{min} : k_m^{max}, k_m^{min} : k_m^{max}\right) \tag{21}$$

The matrix $\mathbf{R}_m'$ is a "wide" matrix of dimension $N_m \times M$ where $N_m = k_m^{max} - k_m^{min} + 1$ and $M \geq N_m$. We underscore that $\mathbf{R}_m^t \neq \mathbf{R}_m'$; the former is a square matrix of dimension $N_m \times N_m$. We observe that the truncated block equalizer is slightly more practical than the partial block equalizer as one does not need to change the front-end matched filter processing as much for each symbol.

Let us now design the MMSE equalizer based on the signal model developed in (17)-(21). Due to the "wide" nature of $\mathbf{R}_m'$, the MMSE equalizer basically consists of a regularized inverse of $\mathbf{R}_m'$ (see *e.g.* [15]), that is, we employ the following equalizer:

$$\mathbf{P}_m^{RT} = \left(\mathbf{R}_m'^{\,H} \mathbf{R}_m^{t\,-1} \mathbf{R}_m' + \sigma^2 \mathbf{I}\right)^{-1} \mathbf{R}_m'^{\,H} \mathbf{R}_m^{t\,-1} \tag{22}$$

$$= \mathbf{R}_m'^{\,H}(\mathbf{R}_m'\mathbf{R}_m'^{\,H} + \sigma^2 \mathbf{R}_m^t)^{-1}, \tag{23}$$

where ^{H} denotes the complex conjugate transpose and $\mathbf{I}$ is the $M \times M$ identity matrix. The related equalizer performance, conditioned on the channel gains, is determined as follows,

$$\mathbf{B}^{RT} = \mathbf{P}_m^{RT}\mathbf{R}_m' \tag{24}$$

$$\mathbf{W}^{RT} = \mathbf{P}_m^{RT}\mathbf{R}_m^t \mathbf{P}_m^{RT\,H}. \tag{25}$$

It is clear that the complexity involved in (23) is smaller than the one needed to compute (22), due to the dimensions of the matrix that needs to be inverted. However, note that the $M \times M$ matrix inversion in (22) can be reduced in complexity by observing that we invert a scaled identity matrix plus a low-rank matrix. The truncated block equalizer offers near-optimal performance.

D. Path-Combining Equalizer

We further reduce complexity by considering a set of p correlators matched to each path for a particular symbol. However, in contrast to effective channel matched filtering which would be achieved by summing these path filter outputs together, we optimally, in the MMSE sense, combine the

outputs. We form,

$$\hat{y}_m(l) = \int v_m^l{}^*(t) r(t) dt \quad (26)$$

$$\hat{\mathbf{R}}_m(l,c) = \int v_m^l{}^*(t) v_n^k(t) dt \quad (27)$$

$$l, k = 1, \cdots, p, \; n \in \mathcal{M}_m, \; c = k + n(p-1) - k_{\min} + 1$$

$$\hat{\mathbf{y}}_m = \underbrace{\hat{\mathbf{R}}_m \left(\mathbf{I}_{N_m} \otimes \mathbf{1}_p \right)}_{\breve{\mathbf{R}}_m} \mathbf{b} + \hat{\mathbf{n}}_m \quad (28)$$

$$\hat{\mathbf{n}}_m \sim \mathcal{CN} \left(\mathbf{0}, \sigma^2 \hat{\mathbf{R}}_m^p \right) \quad (29)$$

$$\hat{\mathbf{R}}_m^p = \hat{\mathbf{R}}_m(1:p, m(p-1)+1:mp). \quad (30)$$

The MMSE equalizer is given below and the matrices needed for performance computation in (8) follow,

$$\mathbf{P}_m^{PC} = \breve{\mathbf{R}}_m^H \left(\breve{\mathbf{R}}_m \breve{\mathbf{R}}_m^H + \sigma^2 \hat{\mathbf{R}}_m^p \right)^{-1} \quad (31)$$

$$\mathbf{B}^{PC} = \mathbf{P}_m^{PC} \breve{\mathbf{R}}_m \quad (32)$$

$$\mathbf{W}^{PC} = \mathbf{P}_m^{PC} \hat{\mathbf{R}}_m^p \mathbf{P}_m^{PC}{}^H. \quad (33)$$

This equalizer is potentially of significantly less complexity than the prior two suboptimal equalizers as it forms only the matched filter outputs matched to the paths associated with symbol m. The path-combining equalizer does achieve good performance as it introduces degrees of freedom for ISI suppression by using p filters per symbol instead of one as is done in the previous sets of equalizers. One can increase performance (and complexity) by increasing the number of per-path correlators for symbols adjacent to the one of interest and then performing MMSE equalization/path combining on the increased set of path filter outputs. We observe that our path-combining equalizer is distinctly different from the chip-rate per-path MMSE filters of [16], [17] wherein per-path MMSE equalizers are designed for a multiuser multipath scenario and then maximal ratio combining is employed.

E. Performance Comparisons

As a performance comparison, and to underscore the adverse effects of the ISI induced by both multipath and Doppler scaling, we examine the performance of a simple matched filter, that is $\hat{b}(m) = \mathrm{dec}(y(m))$. The performance of the matched filter using a Gaussian approximation is given by (8) with $\mathbf{B}^{MF} = \mathbf{W}^{MF} = \mathbf{R}$. Matched filter performance provides an upper bound to the performance of the various equalizers described above. A lower bound is provided by the *matched filter bound*, which is the optimal filter in the absence of any other bits, but the one of interest. The conditional probability of error is given by,

$$P_e^{mfb}(m|\mathbf{h}) = Q\left(\frac{\sqrt{\mathbf{R}(m,m)}}{\sigma} \right). \quad (34)$$

V. Numerical Results

Our numerical results are semi-analytic, in that we compute the various conditional probabilities of error noted above for a specific channel realization and then average over these realizations. That is, for the demodulation of symbol m,

$$\hat{P}_e(m) = \frac{1}{N} \sum_{i=1}^{N} P_e \left(m | \mathbf{h}(\omega_i) \right),$$

where $\mathbf{h}(\omega_i)$ denotes the i'th realization of the channel. We observe that closed form computation of the performance of the MMSE-based equalizers is challenged by the fact that the matrices to be inverted are a function of the channel gains, which are random. We also observe that our sub-optimal equalizers cannot be meaningfully analyzed by exploiting large block lengths as their window of operation has been designed to be small. Our definition of the signal-to-noise-ratio (SNR) is given as follows, $\mathrm{SNR} = \frac{\mathbb{E}\left[\|\underline{h}\|^2 \right]}{\sigma^2}$. Due to the multi-scale, multi-lag model, there is, in fact, no consistent measure of SNR, as the norm of the effective channel function is changing as a function of time.

We consider a $p = 3$ path system, where the delays are fixed to be: $[0.2T_s, 0.5T_s, 0.8T_s]$ where T_s is the symbol duration which is taken to be 10msec, and a carrier frequency $f_c = 10$kHz. The pulse shape is a square-root raised cosine pulse with a roll-off factor of 10%. We examined data blocks of length $M = 64$. The number of Monte Carlo runs was 500.

In the first set of semi-analytic performance curves, we considered the following Doppler scales: $[0.99, 1.00, 1.01]$, which correspond to a fast fading environment. We note that there is no relationship between delay and Doppler scaling. The memory varied from two to four, with the bulk of the symbols having a channel memory of four symbols. A larger delay spread would increase the memory and thus the complexity of the regularized truncated and partial block equalizers, but not that of the path-combining equalizer. Due to the fact that the middle path has zero delay and is neither compressed nor dilated, the memory initially increases as a function of symbol index, then decreases slightly as the effects of the dilation/compression and the tap delays mutually interact.

Figure 1 depicts the performances of the full, partial, and truncated block equalizers as well as the path-combining equalizer versus the matched filter bound and the performance of the matched filter, which performs no equalization for symbol 32, which is in the middle of the block. We see that the full block equalizer's probability of error is essentially that of the matched filter bound and the truncated and partial block equalizers offer near optimal performance. The path-combining equalizer which of the least complexity by a significant amount has additional minor performance degradation. All equalizers greatly outperform the matched filter. The relative performance of these three suboptimal equalizers is explained as follows: the partial and truncated block equalizers compensate for the additional ISI after the matched filtering with the partial or full channel functions, and it does not seem to make a big difference whether the partial or full channel functions are used. The path-combining equalizer collects all of the signal energy due to the symbol of interest and exploits the p degrees of freedom to perform additional interference
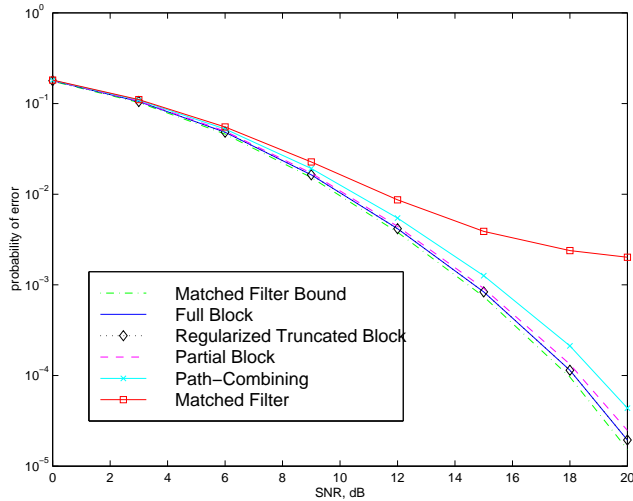
Fig. 1. Average probability of error versus SNR for symbol index $m = 32$, with Doppler scales $[0.99, 1.00, 1.01]$.
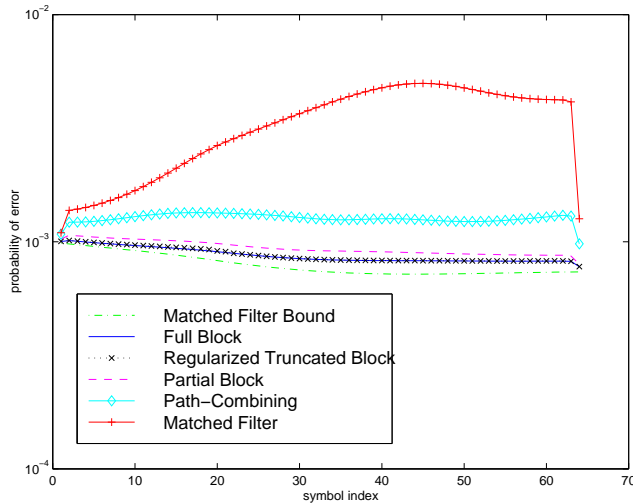

Fig. 2. Average probability of error versus symbol index for SNR = 15dB, with Doppler scales $[0.99, 1.00, 1.01]$.

suppression. Note that the degrees of freedom for the partial and truncated block equalizers, N_m is matched to the number of interfering symbols that must be suppressed.

The performance as a function of the symbol index is shown next for SNR = 15dB in Figure 2. We see that the matched filter and the path-combining equalizer are more sensitive to the symbol index than the other equalizers.

Although not depicted for space considerations, we also examined the Doppler scale scenario: $[0.98, 1.00, 1.02]$; herein, the Doppler spread has been significantly increased. Interestingly, the Doppler scale effects as exhibited in the residual "modulation" behave as spreading functions which orthogonalize the signal contributions due to each path, thus equalization is not as important and all equalizers provide near-optimal performance.

VI. CONCLUSIONS

A major goal of the current work is to introduce the problem of channel equalization for channels which exhibit both multi-lag and multi-scale effects. In such channels, optimized equal-

izers will be time-varying with symbol index. Classical equalizer structures are re-examined and meaningfully modified in the context of such channels. As such, the full, partial and truncated block equalizers are studied, as is a low complexity path-combining equalizer. All equalizer structures greatly outperform the matched filter which does no equalization. We observed that the full block equalizer offers near-optimal performance closely followed by the truncated block equalizer and the partial block equalizer. The path-combining equalizer offers the best tradeoff between complexity and performance.

REFERENCES

[1] I. R. Capoglu, Y. Li, and A. Swami, "Effect of doppler spread in OFDM-based UWB systems," *IEEE Transactions on Wireless Communictations*, vol. 4, no. 5, pp. 2559–2567, Sept 2007.

[2] S.-J. Hwang and P. Schniter, "Efficient communication over highly spread underwater acoustic channels," in *WuWNet '07: Proceedings of the second workshop on Underwater networks*, 2007, pp. 11–18.

[3] Y. V. Zakharov and V. P. Kodanev, "Multipath-Doppler diversity of OFDM signals in an underwater acoustic channel," in *IEEE International Conference on Acoustics, Speech, and Signal Processing*, vol. 5, 2000, pp. 2941–2944.

[4] J. Preisig, "The impact of underwater acoustic channel structure and dynamics on the performance of adaptive coherent equalizers," in *High Frequency Ocean Acoustics*, 2004.

[5] S. T. Rickard, R. V. Balan, H. V. Poor, and S. Verdú, "Canonical time-frequency, time-scale, and frequency-scale representations of time-varying channels," *Communications in Information and Systems*, vol. 5, no. 2, pp. 197–226, 2005.

[6] Y. Jiang and A. Papandreou-Suppappola, "Discrete time-scale characterization of wideband time-varying systems," *IEEE Transactions on Signal Processing*, vol. 54, no. 4, pp. 1364–1375, April 2006.

[7] A. Margetts, P. Schniter, and A. Swami, "Joint scale-lag diversity in wideband mobile direct sequence spread spectrum systems," *IEEE Transactions on Wireless Communications*, vol. 6, no. 12, pp. 4308–4319, December 2007.

[8] B.-S. Chen, Y.-C. Chung, and D.-F. Huang, "A wavelet time-scale deconvolution filter design for nonstationary signal transmission systems through a multipath fading channel," *IEEE Transactions on Signal Processing*, vol. 47, no. 5, pp. 1441 – 1446, May 1999.

[9] S. Yerramalli and U. Mitra, "On optimal resampling for OFDM signaling in doubly-selective underwater acoustic channels," in *OCEANS 2008*, Sept. 2008, pp. 1–6.

[10] ——, "Blind resampling parameter estimation for doubly selective underwater acoustic channels," in *ISCAS 2010*, May 2010, invited paper.

[11] G. Acosta, K. Tokuda, and M. A. Ingram, "Measured joint Doppler-delay power profiles for vehicle-to-vehicle communications at 2.4 ghz," in *Global Telecommunications Conference, 2004. GLOBECOM '04. IEEE*, vol. 6, Nov.-3 Dec. 2004, pp. 3813–3817.

[12] G. Acosta and M. A. Ingram, "Six time- and frequency-selective empirical channel models for vehicular wireless lans," in *1st IEEE International Symposium on Wireless Vehicular Communications*, September 2007.

[13] H. V. Poor and S. Verdú, "Probability of error in mmse multiuser detection," *Information Theory, IEEE Transactions on*, vol. 43, no. 3, pp. 858–871, May 1997.

[14] L. Rugini, P. Banelli, and G. Leus, "Simple equalization of time-varying channels for ofdm," *IEEE Communications Letters*, vol. 9, no. 7, pp. 619–621, July 2005.

[15] L. Rugini, P. P. Banelli, and S. Cacopardi, "A full-rank regularization technique for MMSE detection in multiuser CDMA systems," *IEEE Communications Letters*, vol. 9, no. 1, pp. 34 – 36, January 2005.

[16] S. L. Miller, M. M. L. Honig, and L. B. Milstein, "Performance analysis of MMSE receivers for DS-CDMA in frequency-selective fading channels," *IEEE Transactions on Communications*, vol. 48, no. 11, pp. 1919 – 1929, November 2000.

[17] M. Latva-Aho and M. J. Juntti, "LMMSE detection for DS-CDMA systems in fading channels," *IEEE Transactions on Communications*, vol. 48, no. 2, pp. 194 –199, February 2000.